A correction factor to account for mixing in Ghyben-Herzberg and critical pumping rate approximations of seawater intrusion in coastal aquifers

María Pool[1,2] and Jesús Carrera[2]

Received 19 November 2010; revised 16 February 2011; accepted 23 February 2011; published 7 May 2011.

[1] The classic Ghyben-Herzberg estimate of the depth of the freshwater-saltwater interface together with the Dupuit approximation is a useful tool for developing analytical solutions to many seawater intrusion problems. On the basis of these assumptions, Strack (1976) developed a single-potential theory to calculate critical pumping rates in a coastal pumping scenario. The sharp interface assumption and, in particular, this analytical solution are widely used to study seawater intrusion and the sustainable management of groundwater resources in coastal aquifers. The sharp interface assumption neglects mixing and implicitly assumes that salt water remains static. Consequently, this approximation overestimates the penetration of the saltwater front and underestimates the critical pumping rates that ensure a freshwater supply. We investigate the error introduced by adopting the sharp interface approximation, and we include the effects of dispersion on the formulation of Strack (1976). To this end, we perform numerical three-dimensional variable density flow simulations. We find that Strack's equations can be extended to the case of mixing zone if the density factor is multiplied by an empirically derived dispersion factor $[1 - (\alpha_T/b')^{1/6}]$, where α_T is transverse dispersivity and b' is aquifer thickness. We find that this factor can be used not only to estimate the critical pumping rate but also to correct the Ghyben-Herzberg estimate of the interface depth. Its simplicity facilitates the generalization of sharp interface analytical solutions and good predictions of seawater penetration for a broad range of conditions.

Citation: Pool, M., and J. Carrera (2011), A correction factor to account for mixing in Ghyben-Herzberg and critical pumping rate approximations of seawater intrusion in coastal aquifers, *Water Resour. Res.*, *47*, W05506, doi:10.1029/2010WR010256.

1. Introduction

[2] More than a century ago, *Ghyben* [1888], more appropriately spelled Ghijben, and *Herzberg* [1901] independently observed that the depth of the freshwater-saltwater interface in coastal aquifers is linearly proportional to the elevation of the water table above sea level. Their findings can be explained by assuming that salt water remains static and that pressure is hydrostatic along the vertical, as had been explained by the less known *DuCommun* [1818]. Salt water can be assumed to remain static if it does not mix with fresh water so that the two fluids are separated by a sharp freshwater-seawater interface and flow is steady state (Figure 1). Under these conditions, the depth of the interface is $\xi = h_f/\epsilon$, where h_f is the (freshwater) piezometric head and ϵ is the buoyancy factor given by $\epsilon = (\rho_s - \rho_f)/\rho_f$, with ρ_f and ρ_s the freshwater and seawater densities, respectively. If the relative density of seawater is taken as 1.025, then the depth of the interface below sea level is about 40 times the freshwater head above sea level.

[3] Sharp interface models are widely employed to study seawater intrusion. When used together with the Dupuit approximation, the problem is simplified and the development of analytical solutions is facilitated [see, e.g., *Bakker*, 2003, 2006; *Nordbotten and Celia*, 2006]. A well-known approach is that of *Strack* [1976], who proposed a single potential for fresh and salinized portions of the aquifer, which facilitates solving relatively complex steady state problems. In particular, Strack used this potential to calculate critical pumping rates in coastal aquifers (i.e., the maximum permissible discharge without salinizing the well). The sharp interface assumption and, in particular, this analytical solution constitute the basis for optimization techniques to ensure a freshwater supply and to provide sustainable management of coastal aquifers [see, e.g., *Willis and Finney*, 1988; *Finney et al.*, 1992; *Emch and Yeh*, 1998; *Naji et al.*, 1999; *Cheng et al.*, 2000; *Park and Aral*, 2004; *Reinelt*, 2005; *Reichard and Johnson*, 2005; *Qahman et al.*, 2005; *Park et al.*, 2009; *Mantoglou*, 2003; *Mantoglou et al.*, 2004; *Kourakos and Mantoglou*, 2009] and also to evaluate the efficiency of measures to control seawater intrusion [*Mahesha*, 1996a, 1996b, 1996c; *Abarca et al.*, 2006].

[1]GHS, Department of Geotechnical Engineering and Geosciences, Universitat Politecnica de Catalunya, UPC-Barcelona Tech, Barcelona, Spain.
[2]GHS, Institute of Environmental Assessment and Water Research, CSIC, Barcelona, Spain.

0043-1397/11/2010WR010256

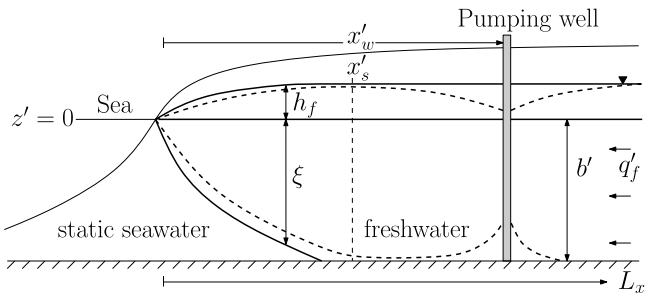

Figure 1. Idealized Ghyben-Herzberg model of the freshwater-saltwater interface in a confined coastal aquifer (solid lines) and the effect of pumping on the interface (dashed lines). Seawater remains static and $\xi \approx 40h_f$, known as the Ghyben-Herzberg approximation.

[4] Unfortunately, the sharp interface assumption neglects mixing of fresh water and seawater, which is one of the most distinctive features of seawater intrusion and its associated dynamics [*Henry*, 1964; *Abarca et al.*, 2007]. In fact, *Gingerich and Voss* [2002] demonstrated that the Ghyben-Herzberg depth is not a good predictor of the depth of potable water because of its failure to deal effectively with the dynamic response of the mixing zone to changes in pumping or rapid recharge. Indeed, the seawater intrusion problem is a three-dimensional phenomenon where a mixing zone develops at the freshwater-seawater interface. Seawater is dispersed across the interface and subsequently is returned to the sea by freshwater discharge, thus forming a convection cell [*Cooper*, 1964]. The loss of seawater energy associated with this flux causes the interface to recede seaward. Therefore, sharp interface approximations are conservative in that they overestimate saltwater penetration[*Dausman et al.*, 2010] and underestimate sustainable pumping rates. Proper accounting of mixing is important not only in determining sustainable management policies but also in analyzing reactions that result from mixing [*Sanford and Konikow*, 1989; *Rezaei et al.*, 2005; *De Simoni et al.*, 2005].

[5] The mixing process is governed by coupled nonlinear equations that describe density-dependent groundwater flow and solute transport. Although transport codes have been developed and tested in recent years to simulate density-dependent flow problems [see, e.g., *Diersch and Kolditz*, 1998; *Voss and Provost*, 2002; *Guo and Langevin*, 2002; *Ackerer et al.*, 1999, 2004], few attempts have been made to simplify modeling seawater intrusion. Thus, a relevant question is whether the sharp interface assumption is suitable for coastal aquifer management, that is, whether the mixing zone and saltwater fluxes can be neglected.

[6] The role and width of the mixing zone in seawater intrusion problems remain a subject of debate. Laboratory experiments typically display narrow mixing zones in homogeneous media [e.g., *Zhang et al.*, 2001; *Volker et al.*, 2002; *Goswami and Clement*, 2007; *Abarca and Clement*, 2009]. However, laboratory experiments are not suitable for representing downscaled versions of any real-world settings. On the other hand, some field studies have found mixing zones ranging from tens to hundreds of meters [*Xue et al.*, 1993; *Price et al.*, 2003; *Langevin*, 2003; *Kim and Chon*, 2007]. However, field measurements are difficult because wells act as short circuits that cause seawater to flow upward along the well, creating artificial salinity profiles in the well. Thus, the freshwater-seawater interface in the boreholes may not represent the interface in the aquifer because the boreholes serve as a means of transferring vertical flow [*Tellam et al.*, 1986; *Kohout*, 1980; *Rushton*, 1980; *Carrera et al.*, 2009]. Accurate and reliable monitoring of seawater intrusion is therefore important [*Shalev et al.*, 2009].

[7] *Abarca et al.* [2007] and *Paster and Dagan* [2007] point out that the width of the mixing zone is controlled mainly by transverse pore-scale dispersion. *Paster and Dagan* [2007] presumed that small transverse pore-scale dispersion calculated from laboratory experiments can create only a relatively narrow mixing zone. They solved the mixing layer problem for seawater intrusion for the upconing problem [*Paster and Dagan*, 2008b] and for 3-D steady flows with an application to a pumping well in a coastal aquifer [*Paster and Dagan*, 2008a]. On the other hand, *Abarca et al.* [2007] demonstrated that both longitudinal and transverse dispersivity contribute to the width of the mixing zone: longitudinal dispersivity controls the width of the mixing zone at the toe of the intrusion wedge, which transfers seaward, and transverse dispersion controls further increase of this width in the midportion of the interface.

[8] Other factors may play a role in the width of the mixing zone. Heterogeneity in the hydraulic conductivity field, which leads to nonuniform advection, may also contribute to enhance mixing. Although *Rahman et al.* [2005], on the basis of laboratory experiments, indicated that heterogeneity has only a minor impact on vertical mixing, *Abarca* [2006] showed that heterogeneity produces a seaward movement of the toe location along with a widening of the mixing zone.

[9] Otherwise, the width of mixing is also influenced by the effects of tidal fluctuations [*Ataie-Ashtiani et al.*, 1999]. Thus, transverse dispersion in coastal aquifers can be driven by wind- or tide-induced sea level fluctuations. *Dentz and Carrera* [2005, 2007] and *Cirpka and Attinger* [2003] adopted a stochastic approach to demonstrate that the interaction between local-scale dispersion and time fluctuations of the flow velocity enhances transverse dispersion. Moreover, *Michael et al.* [2005] used hydraulic gradient measurements to conclude that the inland seasonal hydrologic cycle causes a seasonal mixing zone movement in coastal aquifers. Finally, an alternative explanation for broad mixing zones observed in coastal aquifers has been provided by *Lu et al.* [2009], who showed that the movement of the mixing zone combined with kinetic mass transfer effects may significantly widen the mixing zone.

[10] The original of our objective was to assess the impact of mixing mechanisms on the analytical solution of *Strack* [1976]. As it turned out, results led to a general correction of the Ghyben-Herzberg solution for the depth of the mixing zone.

2. Concepts and Methods

2.1. Problem Statement: Critical Pumping Rate

[11] We consider a homogeneous horizontal confined coastal aquifer of constant thickness $b'[L]$ with a specific freshwater discharge from inland of $q'_f[L\,T^{-1}]$ (Figure 2). A constant flow rate, Q'_w $[L^3T^{-1}]$, is pumped from a fully penetrating well located at a specific distance x'_w $[L]$ from the coast. The ensuing drawdown causes seawater to penetrate farther inland as Q'_w increases. We calculated the pumped water salinity at the well. The critical pumping rate,

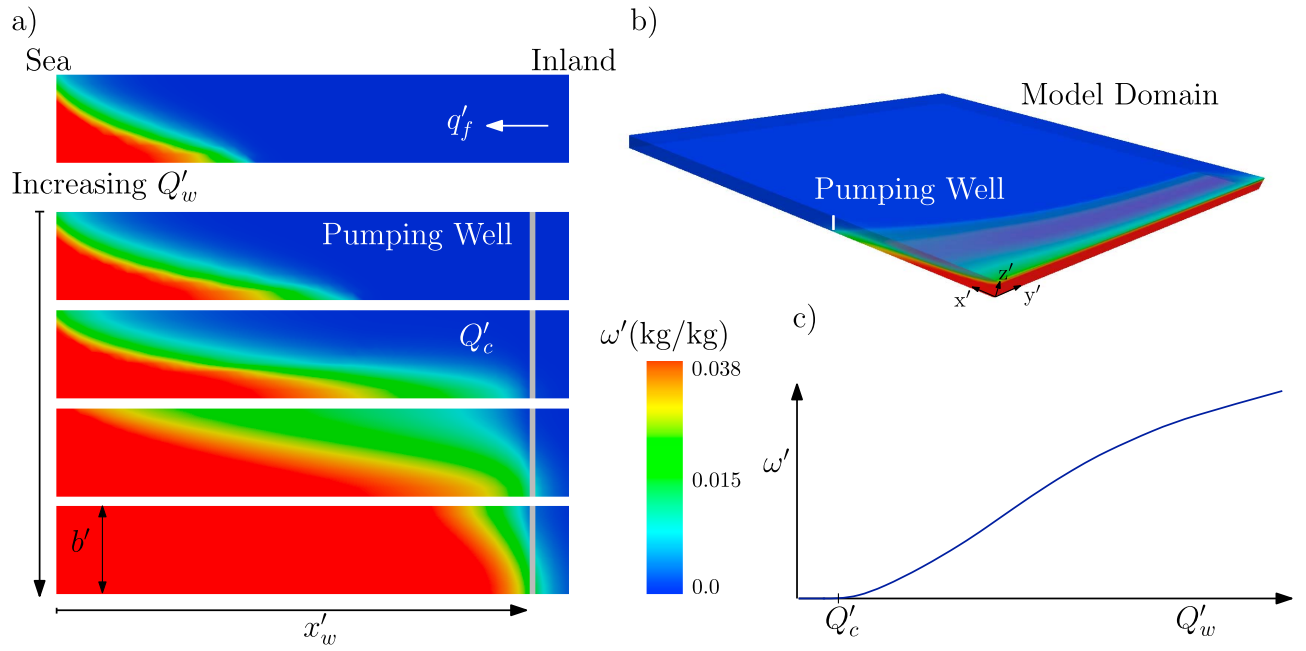

Figure 2. Schematic description of the case study: (a) salt mass fraction distributions in the vertical cross section containing the well for different pumping rates, (b) model domain, and (c) dependence of steady state salinity at the well on pumping rate.

Q'_c [L^3T^{-1}], is defined as the maximum pumping rate with negligible saltwater proportion. Henceforth, a 0.1% of mixing with seawater at the well will be adopted as the salination threshold.

2.2. Governing Equations

[12] Modeling seawater intrusion entails solving the coupled flow and transport equations. Given that these have been described in detail [see, e.g., *Bear*, 1972], we present only their dimensionless form below. Thus, primed variables (e.g., Q'_w) represent physical dimensional variables, whereas the prime is suppressed (e.g., Q_w) for their dimensionless counterparts.

[13] A three-dimensional coordinate system is adopted, with the z' axis pointing vertically upward and the x' axis pointing inland orthogonally to the shore (Figure 1). Dimensionless coordinates are defined as $x = x'/x'_w$, $y = y'/x'_w$, and $z = z'/x'_w$. The dimensionless Darcy's velocity is $\mathbf{q} = \mathbf{q}'/q'_f$, and the dimensionless fluid density is $\rho = \rho'/\rho_s$, where ρ_s is the seawater density and ρ' [$M\,L^{-3}$] is assumed to be a linear function of the salt mass fraction ω' [$M^3\,M^{-3}$] (mass of dissolved salt per unit mass of fluid). Thus, we adopt $\rho' = \rho_f(1 + \epsilon\omega)$, where ω represents the dimensionless salt mass fraction $\omega = \omega'/\omega_s$, which can be viewed as the proportion of seawater, where ω_s is the salt mass fraction in seawater ($\omega_s = 3.86 \times 10^{-2}$ kg kg^{-1}) and ϵ is the buoyancy factor given by $\epsilon = (\rho_s - \rho_f)/\rho_f$, with ρ_f the freshwater density (typical values of ϵ range around 1/40).

[14] Using these definitions, fluid mass conservation in steady state is recast in a dimensionless form, leading to

$$\nabla \cdot (\rho \mathbf{q}) = \rho Q_w \delta(x - x_w, 0) f_w(z), \tag{1}$$

where ∇ expresses the dimensionless form of the del operator; the Dirac's delta δ represents the dimensionless location of the well; the dimensionless function $f_w(z)$ expresses the vertical distribution of extraction, which is assumed to be uniform here ($f_w(z)$ is zero, except in the portion of the aquifer thickness where the well is pumping); and Q_w is the dimensionless pumping rate of the well, defined as $Q_w = Q'_w/(b'x'_w\,q'_f)$.

[15] Equation (1) is solved with the following boundary conditions: specified flux (q'_f) along the inland boundary ($x' = L_x$) and specified equivalent freshwater head along the seaside boundary ($x' = 0$), which in terms of dimensionless variables read as

$$\begin{aligned} \frac{\partial h}{\partial x}\Big|_{x=\frac{L_x}{x'_w}} &= -1 \\ h|_{x=0} &= -\frac{1}{a}z, \end{aligned} \tag{2}$$

respectively, where the dimensionless equivalent freshwater head and the dimensionless number a and are defined by

$$\begin{aligned} h &= \frac{h'K}{x'_w q'_f} \\ a &= \frac{q'_f}{\epsilon\,K}, \end{aligned} \tag{3}$$

where h' [L] is the equivalent freshwater head ($h' = p'/\rho_f g + z'$) and K [$L\,T^{-1}$] is hydraulic conductivity, which is assumed to be isotropic for simplicity. Note that a represents the ratio of freshwater flux to the characteristic buoyancy flux [*Henry*, 1964; *Abarca et al.*, 2007].

[16] Regarding transport, Peclet numbers are employed to describe the relative importance of advective and diffusive and dispersive transport mechanisms:

$$\begin{aligned} d_m &= \frac{D_m\,\phi}{q'_f\,x'_w}, \\ \mathbf{D} &= \frac{\mathbf{D}'}{\alpha_T\,q'_f}, \\ d_p &= \frac{\alpha_T}{x'_w}, \end{aligned} \tag{4}$$

Table 1. Parameters Used in Numerical Simulations

Parameter	Value	Description
K	10 m/d	hydraulic conductivity (isotropic)
b'	50 m	aquifer thickness
x'_w	200, 300, 400 m	distance of the well from the coast
ϕ	0.2	porosity
$\alpha_{L\max,\mathrm{med}}$	10 m	maximum or medium longitudinal dispersivity
$\alpha_{L\min}$	1 m	minimum longitudinal dispersivity
α_T	1 m	transverse dispersivity
D_m	8.6E-5 m^2/d	molecular diffusion coefficient
μ	86.4 kg/m d	freshwater viscosity
q'_f	2.5E-2 m/d	freshwater influx at the inland boundary

where ϕ $[L^3L^{-3}]$ is porosity, D_m $[L^2T^{-1}]$ is the molecular diffusion coefficient, α_T is the transverse dispersivity coefficient $[L]$, and $\mathbf{D}'$ is the dispersion tensor defined by

$$D'_{ij} = \delta_{ij}\alpha_T|\mathbf{q}'| + (\alpha_L - \alpha_T)\frac{q'_i \quad q'_j}{|\mathbf{q}'|} \quad , i,j = x,y,z. \tag{5}$$

With these definitions, the dimensionless form of the transport equation is

$$(\rho\mathbf{q})\cdot\nabla\omega - \nabla\cdot\left[\rho\left(\mathbf{D}\ d_p + d_m\mathbf{I}\right)\nabla\omega\right] = 0, \tag{6}$$

where $\mathbf{I}$ is the identity matrix.

[17] The dimensionless transport equation (6) is subject to a nondispersion boundary condition at the seaside boundary, which is defined as

$$-(\rho\mathbf{q}\omega - \mathbf{D}\nabla\omega)|_{x=0} \ \cdot\ \mathbf{n} = \begin{cases} \rho\mathbf{q}\cdot\mathbf{n}\omega_s & \text{if } \mathbf{q}\cdot\mathbf{n} < 0 \\ \rho\mathbf{q}\cdot\mathbf{n}\omega|_{x=0} & \text{if } \mathbf{q}\cdot\mathbf{n} > 0, \end{cases} \tag{7}$$

where $\mathbf{n}$ is the unit vector normal to the boundary and pointing outward. This implies that the salt mass fraction equals either that of seawater ($\omega = 1$) for inflowing portions of the boundary or that of the resident mass fraction for outflowing portions [*Voss and Souza*, 1987; *Frind*, 1982].

2.3. Sharp Interface Approximation

[18] We review here the analytical solution of *Strack* [1976]. The formulation is based on the Ghyben-Herzberg formula together with the Dupuit approximation. Under these conditions, head is constant along the vertical in the freshwater zone (depends only on x and y) and flux is neglected in the seawater zone (see Figure 1 for the problem setting). Strack's potential Φ allows us to write the flow equation as

$$\nabla_h^2\Phi = 0, \tag{8}$$

where $\nabla_h = (\partial/\partial x', \partial/\partial y')$.

[19] The solution of (8) for a pumping well adjacent to a prescribed potential boundary can be obtained by superimposing two Thiem solutions centered at the well and its image, respectively. Given the specific freshwater discharge from inland and the pumping rate in the well, the interface position ξ can be calculated by

$$\frac{1}{2}K\ \xi^2\ \epsilon = q'_f\ b'\ x' + \frac{Q'_w}{4\pi}\ln\left[\frac{(x'-x'_w)^2+y'^2}{(x'+x'_w)^2+y'^2}\right]. \tag{9}$$

[20] The solution of Φ also allows us to find the streamline that separates water flowing into the well from that flowing into the sea. This streamline becomes stagnant ($q_x = 0$) at the symmetry axis ($y = 0$) at an inland distance (Figure 1):

$$x_s = \left[1 - \frac{Q_w}{\pi}\right]^{1/2}. \tag{10}$$

[21] As the pumping rate at the well increases, the interface migrates landward and the stagnation point migrates seaward. When they cross, seawater enters into the well capture zone and the well becomes salinized. The critical pumping rate $Q'_w = Q'_c$ is found by imposing $\xi = b'$ at $x' = x'_s$. Therefore, inserting (10) into (9) leads to the implicit equation for the critical pumping rate

$$\lambda = 2\left[1 - \frac{Q_c}{\pi}\right]^{1/2} + \frac{Q_c}{\pi}\ \ln\ \frac{\left[1-(1-Q_c/\pi)^{1/2}\right]}{\left[1+(1-Q_c/\pi)^{1/2}\right]}, \tag{11}$$

where Q_c $[Q'_c/(b'x'_w\ q'_f)]$ is the dimensionless critical pumping rate and the dimensionless constant λ is defined by $\lambda = b/a$, where b represents the dimensionless aquifer thickness ($b = b'/x'_w$) and a is defined by equation (3). Note that the critical pumping rate depends exclusively on the following variables: the specific freshwater discharge from inland, the hydraulic conductivity, the aquifer thickness, the distance of the well from the coast, and the buoyancy factor.

2.4. Numerical Methodology

[22] The coupled flow and transport equations are solved in three dimensions to evaluate the critical pumping rates taking mixing into account. A confined coastal aquifer of finite areal extent ($1100 \times 2200 \times 50$ m^3) with a fully penetrating well located at a specific distance from the coast is considered in this study. Owing to the symmetry with respect to the x axis, numerical simulations were carried out in half of the aquifer in order to reduce computations (Figure 2b). Discretization is adjusted to ensure accuracy.

[23] Aquifer parameters are given in Table 1 for the base case. Computer simulations were performed with SUTRA [*Voss and Provost*, 2002]. The simulations were carried out by increasing gradually the constant pumping rate at the well initially under nonpumping conditions. For each test, the pumping rate is constant until steady state.

3. Salinization Mechanism

[24] Under nonpumping conditions, the classic vertical saltwater circulation cell is developed by combining buoyancy forces and hydrodynamic dispersion. Once the well starts pumping, seawater migrates toward the pumping well. A low or moderate pumping rate at the well causes seawater to spread at the bottom of the aquifer, widening the mixing zone in the longitudinal direction. However, the mean flow over the saltwater wedge remains mainly perpendicular to the density gradient. Once the well starts pumping salt water, i.e., when the critical pumping rate Q_c is reached, velocity in the saltwater body increases, thus increasing dispersion and invalidating the static assumption used to calculate the interface location. If the well discharge is further increased, freshwater velocities between the well and the sea are reduced drastically, which leads to a thick tran-

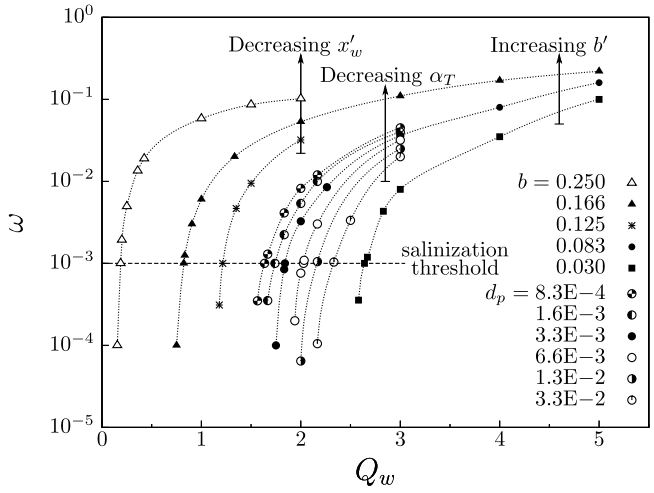

Figure 3. Dimensionless salt mass fraction at the well for a range of pumping rates showing the effect of varying separately distance of the well to the shore, x'_w (base case); aquifer thickness, b' (α_T = 1 m and x'_w = 300 m); and transverse dispersivity, α_T (b' = 25 m and x'_w = 300 m).

sition zone. Finally, a further increase in the pumping rate causes seawater to flow toward the pumping well throughout the entire aquifer thickness. The salination mechanism is illustrated in Figure 2a.

[25] It should be pointed out that when the pumping rate is increased, the shape of the freshwater-seawater interface contrasts with the classic representation obtained by the sharp interface assumption (Figure 1). In particular, upconing does not occur if the entire aquifer thickness is pumped.

[26] Well discharge salinity depends on the pumping rate, the well location, the aquifer thickness, and hydrodynamic dispersion. Needless to say, increasing x_w leads to an increase in the critical pumping rate. Therefore, we consider three different values for x_w, the distance of the well from the coast (see Table 1).

[27] Several sets of simulations were carried out to determine the effects of buoyancy and dispersion on the concentration distribution and critical pumping rate. Runs were performed by varying independently the aquifer thickness (between 9 and 50 m) and the longitudinal and transverse dispersivities (between 10 and 50 m and between 0.25 and 10 m, respectively). Buoyancy effects increase with aquifer thickness, causing the interface to migrate inland. Lateral fluxes around the well also increase as the aquifer thickens. As a result, the thicker the aquifer, the lower the critical pumping rate. Increasing the longitudinal dispersivity causes the mixing zone to broaden seaward at the bottom of the aquifer. In fact, the saline end of the mixing zone moves seaward, while the freshwater end remains unaffected [*Abarca et al.*, 2007]. Therefore, when the longitudinal dispersivity is increased, there is only a slight decrease in the salinity at the well for high pumping rates. Thus, the numerical results suggest that longitudinal dispersivity does not play a major role in the critical pumping rate, which is in line with the results of *Reilly and Goodman* [1987] for the steady state density-dependent upconing problem. On the other hand, increasing transverse dispersivity broadens the mixing zone and displaces the interface seaward, causing a reduction in salinity at the well and increasing the critical pumping rate. Therefore, transverse dispersivity plays a crucial role in controlling the critical pumping rate. Figure 3 illustrates the impact of well location, aquifer thickness, and transverse dispersivity on salinity at the well and, hence, on the critical pumping rate for a range of pumping rates at the well.

[28] It should be pointed out that small changes in pumping rate lead to very large relative changes in salinity (note the logarithmic scale on the ω axis of Figure 3) near the critical pumping rate. Therefore, the critical pumping rate is only marginally sensitive to the actual value of the salinity threshold around 0.1% of mixing with seawater.

[29] The evolution of the saltwater mass flux (SMF) entering from the seaside boundary was studied to further explore the dynamics of a pumping scenario. There have been few studies on the quantification of the SMF in seawater intrusion. *Destouni and Prieto* [2003] proposed a linear relationship between the net land-determined groundwater drainage (total freshwater drainage minus groundwater extraction) and the seawater inflow at the seaside boundary. More recently, *Smith* [2004] found that SMF depends on the geometric average of the principal values of the hydraulic conductivity tensor and on the square root of the transverse dispersivity. This was confirmed by *Abarca et al.* [2007], who showed that seawater flux is essentially proportional to the geometric average of the hydraulic conductivity and $(\alpha_T/b')^{1/3}$ and is independent of prescribed freshwater flux. However, M. Pool et al. (Vertical average for modeling seawater intrusion, submitted to *Water Resources Research*, 2010) demonstrated that prescribed freshwater flux has some effect on SMF. In a pumping scenario, the pumping rate at the well plays a major role in SMF. In fact, SMF depends nonmonotonically on the pumping rate, which seems to be counterintuitive. A low or moderate pumping rate at the well causes the freshwater influx to drift toward the well, but the well capture zone is entirely contained within the freshwater body. This leads to a decrease in the freshwater discharge to the sea and thus to a reduction in dispersion fluxes and the pressure gradient close to the seaside boundary. Therefore, SMF falls although the interface moves inland. At high

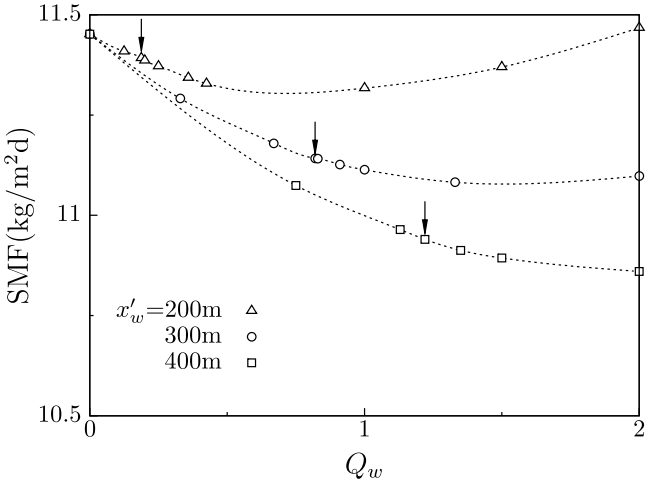

Figure 4. Effect of pumping rate at the well on saltwater mass flux (SMF) for three distances of the well from the coastal boundary (see Table 1 for the parameters). The arrows indicate the critical pumping rate.

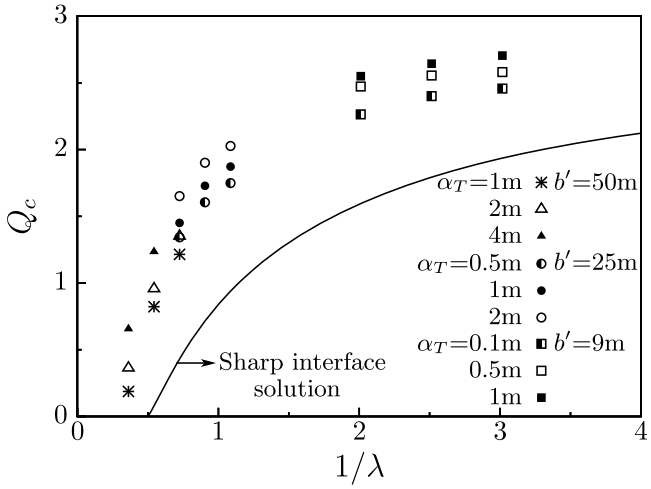

Figure 5. Comparison between analytical and numerical results for the critical pumping rate in terms of the dimensionless constant λ.

pumping rates, the well capture zone would tend to favor lateral fluxes from the seaside boundary to the well. Henceforth, the drawdown generated by pumping causes seawater to penetrate further inland along the boundary with an increase in SMF. This is particularly noticeable when the well is located farther from the coast. This effect is illustrated in Figure 4, which depicts SMF when the pumping rate is increased in a well located at different distances from the seaside boundary.

4. Comparison Between Analytical and Numerical Results

[30] Critical pumping rates obtained with Strack's equation (equation (11)) are compared with solutions from the dispersive models in Figure 5. Although the solutions of the two models follow a similar trend as a function of λ (equation (11)), the results are different. As expected, the differences between the critical pumping rate of the two models become more pronounced in thick aquifers as a result of density differences. Needless to say, the discrepancy between the numerical and analytical results increases with increasing transverse dispersivity. Neglecting mixing, the sharp-interface approximation overestimates seawater penetration and therefore underestimates the critical pumping rates. This result agrees with the findings of *Reilly and Goodman* [1987] and *Zhou et al.* [2005] for the classical problem of saltwater upconing under a pumping well.

5. Empirical Correction

[31] A procedure to acknowledge mixing when determining the critical pumping rate in coastal aquifers is outlined below. We define λ_{num} by substituting the numerical results of Q_c in equation (11). We then evaluate the deviation of λ_{num} from λ and use an optimal regression model to identify the parameters that best explain this deviation so as to obtain a simple empirical correction for the critical pumping rate.

[32] We used the algorithm of *Furnival and Wilson* [1974] to find the best subset regressions with independent candidate variables. The routine eliminates some subsets of candidate variables by obtaining lower bounds on the error sum of squares from fitting larger models. Basically, the dimensionless parameters defined in section 2.2 are proposed as independent variables for the regression model. The equation that best represents the deviation is shown in Figure 6.

[33] As expected, the deviation of λ_{num} from λ is due to dispersion, and, consequently, this deviation is sensitive to transverse dispersivity and aquifer thickness. Therefore, we propose to continue using equation (11) to estimate Q_c but replacing λ by

$$\lambda_d = \frac{\epsilon^* K b'}{q'_f x'_w}, \tag{12}$$

where the only difference with respect to the original definition of λ lies in ϵ^*, which modifies ϵ to account for mixing as

$$\epsilon^* = \epsilon\left[1 - \left(\frac{\alpha_T}{b'}\right)^{1/6}\right]. \tag{13}$$

[34] Figure 7 illustrates the validity of equation (12) by displaying the dimensionless critical pumping rates with respect to the dispersive constant λ_d for different aquifer thickness and transverse dispersivity values. Note that the analytical solution with the correction factor predicts quite accurately the critical pumping rates obtained, acknowledging mixing for a broad range of conditions.

[35] The fact that the correction in equation (13) captures the effect of mixing on the critical pumping rate suggests that it may also be used to represent the depth of the interface. Therefore, we rewrite the Ghyben-Herzberg approximation to the interface depth as

$$\xi = \frac{h_f}{\epsilon^*}. \tag{14}$$

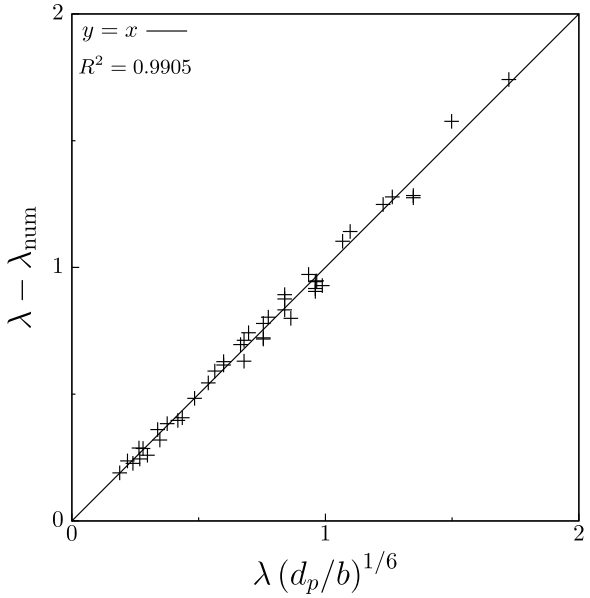

Figure 6. Regressions obtained for the deviation of numerical results from λ resulting from the analytical pumping rates of Strack's equation.

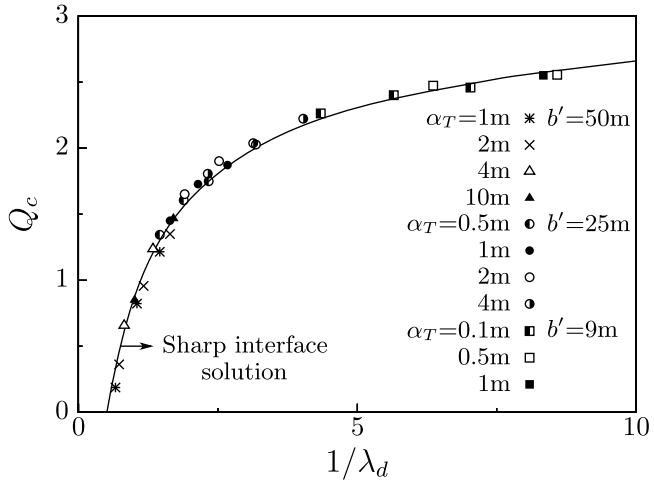

Figure 7. Dimensionless critical pumping rates versus the dispersive constant λ_d ($\lambda_d = \epsilon^* K b'/q'_f x'_w$) with $\epsilon^* = \epsilon [1 - (\alpha_T/b')^{1/6}]$.

The validity of this formulation is corroborated by comparing the salt mass fraction distributions derived from numerical models and the results from the corrected analytical solution. Accordingly, we consider an aquifer of thickness of $b' = 25$ m and transverse dispersivity of $\alpha_T = 0.25$ m with a fully penetrating well located at $x'_w = 300$ m from the coast. The pumping rate at the well Q_w is increased until the critical pumping rate Q_c. As shown in Figure 8, the proposed correction predicts quite accurately the most saline portion (between 50% and 75% mixing ratios) of the mixing zone.

[36] The fact that dispersivity is raised to the power of 1/6 implies that the correction term becomes relevant even for very small dispersivities. This is illustrated in Figure 9, which displays the toe location and the critical pumping rate for the conditions described by *Cheng et al.* [2000] for a single pumping well. It is noted that the critical pumping rate varies substantially in response to transverse dispersivity.

6. Summary and Conclusions

[37] Sharp interface models are widely used to study seawater intrusion. However, the sharp interface approach neglects mixing, thus overestimating the position of the saltwater front and underestimating the critical pumping rates.

[38] We investigated the error introduced by adopting the sharp interface approximation as well as its impact on seawater intrusion. We conclude that accurate results can be obtained using Strack's equations with a simple empirically derived correction factor that depends only on transverse dispersivity and aquifer thickness: $\epsilon^* = \epsilon[1 - (\alpha_T/b')^{1/6}]$. Example calculations demonstrate that excellent results are obtained when using sharp interface approximations (such as Ghyben-Herzberg or Strack's) with ϵ^* instead of ϵ. Depth to the interface computed using the Ghyben-Herzberg equation with ϵ^* identifies the actual depth of the most saline portion of the mixing zone (mixing ratios between 50% and 75% of seawater). This is unimportant when the mixing zone is narrow but implies that the proposed equation should be used with care when it is broad because significant salinities will be found above the computed depth. The correction factor allows us to generalize sharp interface results and leads to quite accurate predictions of seawater penetration for a broad range of conditions. The correction factor may be applied in two ways. First, it can be used to develop optimization techniques to provide sustainable management of groundwater resources in coastal aquifers. Second, it may be employed to compute the extent

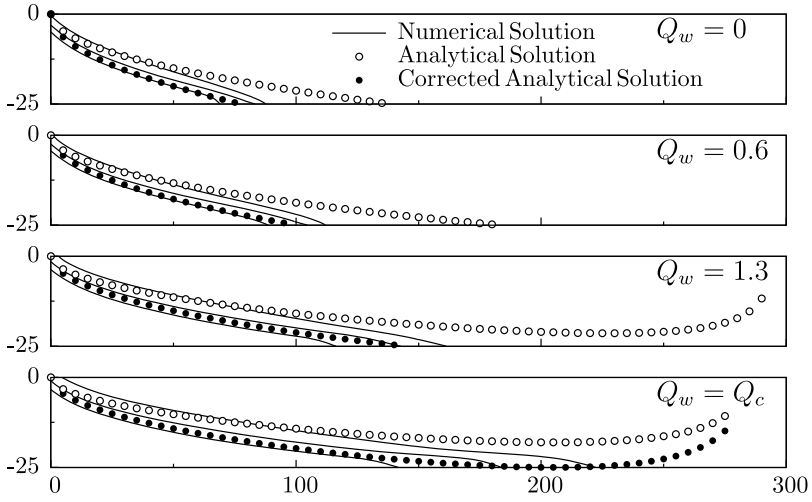

Figure 8. Profiles of seawater intrusion along the vertical plane perpendicular to the coast of an aquifer of thickness of $b' = 25$ m and transverse dispersivity of $\alpha_T = 0.25$ m with a fully penetrating well located at $x'_w = 300$ m from the coast. We show the numerical solution to the problem (the solid lines represent isoconcentration lines of 25%, 50%, and 75% mixing ratios), the Ghyben-Herzberg sharp interface solution (equation (9), $\xi = h_f/\epsilon$, open dots), and the solution obtained with the proposed approximation (equation (9), $\xi = h_f/\epsilon^*$ with $\epsilon^* = \epsilon [1 - (\alpha_T/b')^{1/6}]$, solid dots) when the pumping rate at the well ($Q_w = Q'_w/x'_w\ b'\ q'_f$) is increased until the critical pumping rate is reached ($Q_c = Q'_c/x'_w\ b'\ q'_f$). Note that the proposed solution approximates fairly well the high-salinity isolines.

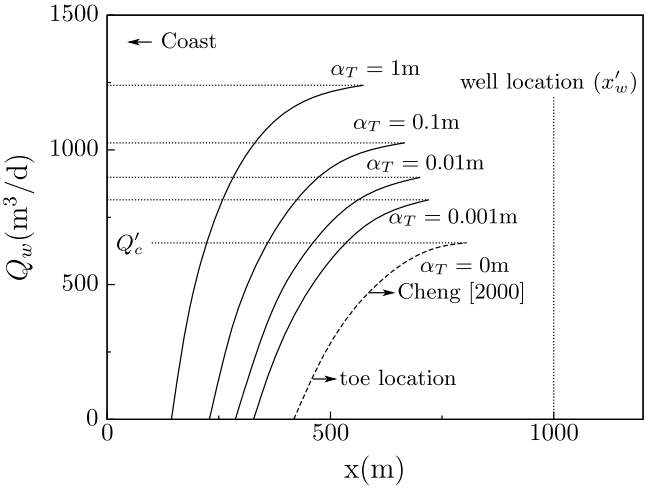

Figure 9. Pumping rate (vertical axis) as a function of prescribed toe location for several values of α_T. The well is located at x'_w = 1000 m from the coast in an unconfined aquifer of thickness b' = 14 m and hydraulic conductivity K = 100 m/d. The critical pumping rate, indicated by the dotted lines, increases dramatically with moderate increases in α_T. In fact, small changes in α_T cause large changes in toe location for any given pumping rate.

of saltwater intrusion. This corrected analytical solution could have important implications for a more realistic and a more effective management of coastal aquifers.

[39] **Acknowledgments.** The first author gratefully acknowledges the receipt of an FI award from the autonomous government of Catalonia for the period during which this work was carried out. We would also like to thank the associate editor and the reviewers for their constructive comments, which significantly improved the manuscript quality.

References

Abarca, E. (2006), Seawater intrusion in complex geological environments, Ph.D. thesis, Tech. Univ. of Catalonia, Barcelona, Spain.

Abarca, E., and T. P. Clement (2009), A novel approach for characterizing the mixing zone of a saltwater wedge, *Geophys. Res. Lett.*, *36*, L06402, doi:10.1029/2008GL036995.

Abarca, E., E. Vázquez-Suñé, J. Carrera, B. Capino, D. Gámez, and F. Batlle (2006), Optimal design of measures to correct seawater intrusion, *Water Resour. Res.*, *42*, W09415, doi:10.1029/2005WR004524.

Abarca, E., J. Carrera, X. Sanchez-Vila, and M. Dentz (2007), Anisotropic dispersive Henry problem, *Adv. Water Resour.*, *30*, 913–926.

Ackerer, P., A. Younes, and R. Mose (1999), Modeling variable density flow and solute transport in porous medium: 1. Numerical model and verification, *Transp. Porous Media*, *35*(3), 345–373.

Ackerer, P., A. Younes, and M. Mancip (2004), A new coupling algorithm for density-driven flow in porous media, *Geophys. Res. Lett.*, *31*, L12506, doi:10.1029/2004GL019496.

Ataie-Ashtiani, B., R. E. Volker, and D. A. Lockington (1999), Tidal effects on sea water intrusion in unconfined aquifers, *J. Hydrol.*, *216*(1–2), 17–31.

Bakker, M. (2003), A Dupuit formulation for modeling seawater intrusion in regional aquifer systems, *Water Resour. Res.*, *39*(5), 1131, doi:10.1029/2002WR001710.

Bakker, M. (2006), Analytic solutions for interface flow in combined confined and semiconfined, coastal aquifers, *Adv. Water Resour.*, *29*, 417–425.

Bear, J. (1972), *Dynamics of Fluids in Porous Media*, 764 pp., Elsevier, Amsterdam.

Carrera, J., J. J. Hidalgo, L. J. Slooten, and Vázquez-Suñé (2009), Computational and conceptual issues in the calibration of seawater intrusion models, *Hydrogeol. J.*, *18*(1), 131–145, doi:10.1007/s10040-009-0524-1.

Cheng, A. H. D., D. Halhal, A. Naji, and D. Ouazar (2000), Pumping optimization in saltwater-intruded coastal aquifers, *Water Resour. Res.*, *36*(8), 2155–2165.

Cirpka, O. A., and S. Attinger (2003), Effective dispersion in heterogeneous media under random transient flow conditions, *Water Resour. Res.*, *39*(9), 1257, doi:10.1029/2002WR001931.

Cooper, J. H. H. (1964), A hypothesis concerning the dynamic balance of fresh water and salt water in a coastal aquifer, *U.S. Geol. Surv. Water Supply Pap., 1613-C*.

Dausman, A., C. Langevin, M. Bakker, and F. Schaars (2010), A comparison between SWI and SEAWAT—The importance of dispersion, inversion and vertical anisotropy, paper presented at the 21st Salt Water Intrusion Meeting, Gov. of Azores, Azores.

De Simoni, M., J. Carrera, X. Sanchez-Vila, and A. Guadagnini (2005), A procedure for the solution of multicomponent reactive transport problems, *Water Resour. Res.*, *41*, W11410, doi:10.1029/2005WR004056.

Dentz, M., and J. Carrera (2005), Effective solute transport in temporally fluctuating flow through heterogeneous media, *Water Resour. Res.*, *40*, W08414, doi:10.1029/2004WR003571.

Dentz, M., and J. Carrera (2007), Mixing and spreading in stratified flow, *Phys. Fluids*, *19*(1), 017107.

Destouni, G., and C. Prieto (2003), On the possibility for generic modeling of submarine groundwater discharge, *Biogeochemistry*, *66*(1–2), 171–186.

Diersch, H.-J. G., and O. Kolditz (1998), Coupled groundwater flow and transport: 2. Thermohaline and 3D convection systems, *Adv. Water Resour.*, *21*, 401–425.

DuCommun, J. (1818), On the cause of fresh water springs and fountains, *Am. J. Sci.*, *14*, 174–176.

Emch, P., and W. Yeh (1998), Management model for conjunctive use of coastal surface water and ground water, *J. Water Resour. Plann. Manage.*, *124*(3), 129–139.

Finney, B. A., Samsuhadi, and R. Willis (1992), Quasi-3-dimensional optimization model of Jakarta basin, *J. Water Resour. Plann. Manage.*, *118*(1), 18–31.

Frind, E. (1982), Simulation of long-term transient density-dependent transport in groundwater, *Adv. Water Resour.*, *5*, 73–88.

Furnival, G., and R. J. Wilson (1974), Regression by leaps and bounds, *Technometrics*, *16*, 499–512.

Ghyben, B. W. (1888), Nota in Verband met de Voorgenomen Putboring Nabij Amsterdam, Amsterdam, *Tijdschr. Kon. Inst. Ing.*, *9*, 8–22.

Gingerich, S., and C. Voss (2002), Three-dimensional variable-density flow simulation of a coastal aquifer in southern Oahu, Hawaii, USA, in *Proceedings SWIM17 Delft 2002*, edited by R. Boekelman, pp. 93–103, Delft Univ. of Technol., Delft, Netherlands.

Goswami, R. R., and T. P. Clement (2007), Laboratory-scale investigation of saltwater intrusion dynamics, *Water Resour. Res.*, *43*, W04418, doi:10.1029/2006WR005151.

Guo, W., and C. Langevin (2002), SEAWAT—User's guide to SEAWAT: A computer program for simulation of three-dimensional varible-density ground-water flow, *Tech. Water Resour. Invest.*, *Book 6*, *Chap. A7*, 77 pp.

Henry, H. R. (1964), Effects of dispersion on salt encroachment in coastal aquifers, *U.S. Geol. Surv. Water Supply Pap., 1613-C*.

Herzberg, A. (1901), Die Wasserversorgung einiger Nordseebäder, *J. Gasbeleucht. Wasserversorg.*, *44*, 815–819, 842–844.

Kohout, F. A. (1980), Differing positions of saline interfaces in aquifers and observation boreholes—Comments, *J. Hydrol.*, *48*(1–2), 191–195.

Kourakos, G., and A. Mantoglou (2009), Pumping optimization of coastal aquifers based on evolutionary algorithms and surrogate modular neural network models, *Adv. Water Resour.*, *32*, 507–521.

Kim, K.-H. P., and C.-M. Chon (2007), A simple method for locating the freshwater-saltwater interface using pressure data, *Groundwater*, *45*, 723–728.

Langevin, C. D. (2003), Simulation of submarine ground water discharge to a marine estuary: Biscayne Bay, Florida, *Ground Water*, *41*(6), 758–771.

Lu, C., P. K. Kitanidis, and J. Luo (2009), Effects of kinetic mass transfer and transient flow conditions on widening mixing zones in coastal aquifers, *Water Resour. Res.*, *45*, W12402, doi:10.1029/2008WR007643.

Mahesha, A. (1996a), Transient effect of battery of injection wells on seawater intrusion, *J. Hydraul. Eng.*, *122*(5), 266–271.

Mahesha, A. (1996b), Steady-state effect of freshwater injection on seawater intrusion, *J. Irrig. Drain. Eng.*, *122*(3), 149–154.

Mahesha, A. (1996c), Control of seawater intrusion through injection-extraction well system, *J. Irrig. Drain. Eng.*, *122*(5), 314–317.

Mantoglou, A. (2003), Pumping management of coastal aquifers using analytical models of saltwater intrusion, *Water Resour. Res.*, *39*(12), 1335, doi:10.1029/2002WR001891.

Mantoglou, A., M. Papantoniou, and P. Giannoulopoulos (2004), Management of coastal aquifers based on nonlinear optimization and evolutionary algorithms, *J. Hydrol.*, *297*(1–4), 209–228.

Michael, H. A., A. E. Mulligan, and C. F. Harvey (2005), Seasonal oscillations in water exchange between aquifers and the coastal ocean, *Nature*, *436*(6), 1145–1148.

Naji, A., A. B. D. Cheng, and D. Ouazar (1999), BEM solution of stochastic seawater intrusion problems, *Eng. Anal. Boundary Elements*, *23*(7), 529–537.

Nordbotten, J. M., and M. A. Celia (2006), An improved analytical solution for interface upconing around a well, *Water Resour. Res.*, *42*, W08433, doi:10.1029/2005WR004738.

Park, C., and M. Aral (2004), Multi-objective optimization of pumping rates and well placement in coastal aquifers, *J. Hydrol.*, *290*(1–2), 80–99.

Park, N., L. Cui, and L. Shi (2009), Analytical design curves to maximize pumping or minimize injection in coastal aquifers, *Ground Water*, *47*(6), 797–805.

Paster, A., and G. Dagan (2007), Mixing at the interface between two fluids in porous media: A boundary-layer solution, *J. Fluid Mech.*, *584*, 455–472.

Paster, A., and G. Dagan (2008a), Mixing at the interface between fresh and salt waters in 3D steady flow with application to a pumping well in a coastal aquifer, *Adv.Water Resour.*, *31*(12), 1565–1577.

Paster, A., and G. Dagan (2008b), Mixing at the interface between two fluids in aquifer well upconing steady flow, *Water Resour. Res.*, *44*, W05408, doi:10.1029/2007WR006510.

Price, R. M., Z. Top, J. D. Happell, and P. K. Swart (2003), Use of tritium and helium to define groundwater flow conditions in Everglades National Park, *Water Resour. Res.*, *39*(9), 1267, doi:10.1029/2002WR001929.

Qahman, K., A. Larabi, D. Ouazar, A. Naji, and A. Cheng (2005), Optimal and sustainable extraction of groundwater in coastal aquifers, *Stochastic Environ. Risk A*, *19*(2), 99–110.

Rahman, A., S. C. Jose, and W. N. O. A. Cirpka (2005), Experiments on vertical transverse mixing in a large-scale heterogeneous model aquifer, *J. Contam. Hydrol.*, *80*, 130–148.

Reichard, E., and T. Johnson (2005), Assessment of regional management strategies for controlling seawater intrusion, *J. Water Resour. Plann. Manage.*, *131*(4), 280–291.

Reilly, T. E., and A. S. Goodman (1987), Analysis of saltwater upconing beneath a pumping well, *J. Hydrol.*, *89*(3–4), 169–204.

Reinelt, P. (2005), Seawater intrusion policy analysis with a numerical spatially heterogeneous dynamic optimization model, *Water Resour. Res.*, *41*, W05006, doi:10.1029/2004WR003111.

Rezaei, M., E. Sanz, E. Raeisi, E. Vázquez-Suñé, C. Ayora, and J. Carrera (2005), Reactive transport modeling of calcite dissolution in the saltwater mixing zone, *J. Hydrol.*, *311*(1–4), 282–298.

Rushton, K. R. (1980), Differing positions of saline interfaces in aquifers and observation boreholes, *J. Hydrol.*, *48*(1–2), 185–189.

Sanford, W. E., and L. F. Konikow (1989), Simulation of calcite dissolution and porosity changes in saltwater mixing zones in coastal aquifers, *Water Resour. Res.*, *25*, 655–667.

Shalev, E., A. Lazar, S. Wollman, S. Kington, Y. Yechieli, and H. Gvirtzman (2009), Biased monitoring of fresh water–salt water mixing zone in coastal aquifers, *Ground Water*, *47*(1), 49–56, doi:10.1111/j.1745-6584.2008.00502.x.

Smith, A. J. (2004), Mixed convection and density-dependent seawater circulation in coastal aquifers, *Water Resour. Res.*, *40*, W08309, doi:10.1029/2003WR002977.

Strack, O. D. L. (1976), A single-potential solution for regional interface problems in coastal aquifers, *Water Resour. Res.*, *12*, 1165–1174.

Tellam, J. H., J. W. Lloyd, and M. Walters (1986), The morphology of a saline groundwater body: Its investigation, description and possible explanation, *J. Hydrol.*, *83*(1–2), 1–21.

Volker, R. E., Q. Zhang, and D. A. Lockington (2002), Numerical modelling of contaminant transport in coastal aquifers, *Math. Comput. Simul.*, *55*, 35–44.

Voss, C. I., and A. Provost (2002), SUTRA, a model for saturated-unsaturated variable-density ground-water flow with solute or energy transport, *U.S. Geol. Surv. Water Resour. Invest. Rep., 02-4231*.

Voss, C. I., and W. R. Souza (1987), Variable density flow and transport simulation of regional aquifers containing a narrow freshwater-saltwater transition zone, *Water Resour. Res.*, *26*, 2097–2106.

Willis, R., and B. Finney (1988), Planning-model for optimal-control of saltwater intrusion, *J. Water Resour. Plann. Manage.*, *114*(2), 163–178.

Xue, Y. Q., J. Wu, P. M. Liu, J. J. Wang, G. Q. B. Jiang, and H. W. Shi (1993), Sea-water intrusion in the coastal area of Laizhou Bay, China: 1. distribution of sea-water intrusion and its hydrochemical characteristics, *Ground Water*, *31*(4), 532–537.

Zhang, Q., R. Volker, and D. Lockington (2001), Influence of seaward boundary condition on contaminant transport in unconfined coastal aquifers, *J. Contam. Hydrol.*, *49*(3–4), 201–215.

Zhou, Q., J. Bear, and J. Bensabat (2005), Saltwater upconing and decay beneath a well pumping above an interface zone, *Transp. Porous Media*, *61*(3), 337–363.

J. Carrera, GHS, Institute of Environmental Assessment and Water Research, CSIC, 18, E-08034, Barcelona, Spain.

M. Pool, GHS, Department of Geotechnical Engineering and Geosciences, Universitat Politecnica de Catalunya, UPC-Barcelona Tech, Jordi Girona 1-3, E-08034, Barcelona, Spain. (maria.pool@idaea.csic.es)